"CH"/N Substituted *mer*-Gaq3 and *mer*-Alq3 Derivatives: An Effective Approach for the Tuning of Emitting Color

Godefroid Gahungu and Jingping Zhang*

Faculty of Chemistry, Northeast Normal University, Changchun 130024, People's Republic of China

Received: April 29, 2005; In Final Form: July 18, 2005

Equilibrium geometry configurations of the "CH"/N substituted Alq3 and Gaq3 derivatives are calculated by density functional theory (B3LYP/6-31G*). The frontier molecular orbital and gap energy calculations for all complexes have been performed at the HF/6-31G* level. It was shown that, compared to the pristine molecules, the HOMO and LUMO are stabilized, the net effect being however an increasing/decreasing of the gap (E_g) depending on the position of the substituted group. On the basis of the equilibrium geometries, the effect of the substitution on the absorption and emission spectra was evaluated using TDB3LYP/3-21G*. It was shown that the change of "CH"/N substituted position on 8-hydroxyquinoline ligand is a powerful approach for the tuning of emitting color. An important blue shift was predicted for 5-substituted 8-hydroxyquinoline derivatives, an important red one being observed for 4-substituted ones. Interestingly, relatively significant blue and red shifts were also predicted for the 7- and 2-substituted derivatives. In this work, the correlation between the spectrum shifts and the metal−ligand bonding is also discussed.

1. Introduction

The best way to alter the $\pi \rightarrow \pi^*$ transition without distorting the molecular shape of the organic light-emitting device (OLED) tris(8-hydroxyquinolinato)aluminum (Alq3), was reported to be a heteroatom incorporation into the 8-hydroxyquinoline ring system.[1] As already known, substitution of an electron-withdrawing substituent/electron-donating at C-5 and C-7 positions (phenoxide side)/C-4 and C-2 positions (pyridyl side) is expected to induce a blue/red shift.[2] A synthesis of two examples of such ligands (4-hydroxy-1,5-naphthyridine and 5-hydroxyquinoxaline resulting from a "CH"/N substitution at positions 4 and 5 of 8-hydroxiquinoline based Al complexes) was reported.[1,2] By use of the ZINDO semiempirical method, a blue-shift emission (ca. 90 nm) relative to Alq3 was predicted for the former,[1] while with the same method, a red-shift absorption (ca. 60 nm) in agreement with experiment (of 57 nm) was predicted for the latter.[3] However, little information can be found in the literature about the other possible "CH"/N substituted derivatives, and even for those already experimentally isolated, some properties such as the dipole moment are not reported yet.

In this contribution, we report on the investigation we have carried out on the effect of the "CH"/N substitution on a set of properties including the dipole moment, absorption and emission spectra relative to those of the pristine Mq3 (M = Ga, Al) complexes. In addition, on the basis of the structural changes induced by the substitution in the geometrical parameters involving the central atom, an investigation of the relationship between the metal−nitrogen bond length and fluorescent spectra has been attempted. The computational results are compared to available theoretical and experimental data.[1−3]

2. Computational Methods

All the geometry optimizations for the ground state (S_0) were performed using Becke's three-parameter hybrid functional[4] combined with the Lee, Yang, and Parr (LYP) correlation functional,[5] denoted B3LYP,[6] with the 6-31G*[7−10] basis set while Hartree−Fock (HF) theory combined to the same basis set was used in a single point calculation to predict the orbital energies.

The low-lying excited-state structure (S_1) was then optimized using the ab initio CIS (configuration interaction with single excitations),[11] the absorption and emission energy being calculated using TD-B3LYP to obtain estimates including some account of electron correlation. In this case, 6-31G[8,9] and 3-21G*[12−14] were used.

All the computational results have been performed using the Gaussian 98 A.9 package,[15] GaussSum[16] being used in electronic transition analysis.

3. Results and Discussion

3.1. Ground States. 3.1.1. Molecular Geometries. The molecular models used in our calculations, obtained by a systematic substitution of "CH" groups with N atoms in positions 2, 3, ..., 7 (see labeling scheme) in each ligand are shown in Figure 1. In the following, the results are presented according to the labeling defined in the same Figure. In Table 1, we give selected geometrical parameters of the Mq3 (M = Al, Ga) derivatives (ML3) together with their corresponding pristine molecules, where both optimized (at the same level of theory) and experimental results[17,18] are listed for comparison. From these results, a same trend is observed for M−N and M−O bond length variations in the two series of derivatives. The former is predicted to be lengthened in MZ3, MX3, and M-6N3, the greatest increase being found to be 0.016 Å, and shortened in the other three cases within 0.019 Å of greatest decrease (observed for MC3). The M−O bond is predicted to be generally slightly lengthened in M-5N3 and M-6N3 (by at most 0.011 Å) and slightly shortened in the other cases (by at most 0.009 Å). These results are in a good agreement with the reported single-crystal X-ray analyses of both Alq3 and Al-5N3 confirm-

10.1021/jp052220a CCC: $30.25
Published on Web 08/27/2005

TABLE 1: Selected B3LYP/6-31G* Optimized Bond Lengths (*R*) and Bond Angles (φ) for "CH"/H Substituted *mer*-AlL3 and *mer*-GaL3 Together with Their Pristine Molecules

R (Å) φ (deg)	Mq3	MC3	MZ3	MX3	M-5N3	M-6N3	M-7N3	exptl[a,b]
				M = Al				
$M-N_A$	2.084	2.071	2.088	2.091	2.079	2.089	2.082	2.050
$M-N_B$	2.126	2.107	2.128	2.142	2.112	2.135	2.127	2.087
$M-N_C$	2.064	2.075	2.070	2.073	2.062	2.068	2.061	2.017
$M-O_A$	1.855	1.875	1.858	1.850	1.866	1.856	1.854	1.850
$M-O_B$	1.881	1.872	1.880	1.874	1.891	1.883	1.881	1.860
$M-O_C$	1.884	1.879	1.885	1.879	1.893	1.886	1.883	1.857
N_A-M-N_C	171.531	170.685	171.329	171.734	171.676	171.847	171.314	173.82
N_B-M-O_A	172.572	172.728	173.003	172.961	173.135	173.195	173.115	171.46
O_C-M-O_B	166.564	166.543	167.003	165.876	167.871	166.281	165.701	168.22
μ^c	4.4693	2.6815	1.1545	2.5428	3.7254	6.5731	7.3205	
$\mu.^d$	5.4703	3.6012	2.1896	3.6041	4.5413	7.8341	8.4061	
				M = Ga				
$M-N_A$	2.097	2.077	2.099	2.105	2.093	2.103	2.097	2.093
$M-N_B$	2.111	2.099	2.112	2.124	2.101	2.119	2.114	2.112
$M-N_C$	2.077	2.088	2.081	2.086	2.074	2.082	2.074	2.092
$M-O_A$	1.934	1.950	1.937	1.929	1.944	1.935	1.933	1.937
$M-O_B$	1.951	1.946	1.950	1.945	1.960	1.952	1.951	1.940
$M-O_C$	1.951	1.946	1.952	1.946	1.961	1.953	1.950	1.965
N_A-M-N_C	167.643	167.971	167.594	167.946	167.775	168.036	167.096	171.300
N_B-M-O_A	171.541	171.764	172.013	171.748	171.814	172.072	171.755	171.300
O_C-M-O_B	165.826	172.714	166.509	165.362	166.887	165.485	164.444	168.000
μ^c	4.4457	2.7801	1.3862	2.6377	3.7800	6.5344	7.0958	
μ^d	5.2900	3.7770	2.4127	3.7659	4.6805	7.8255	8.2742	

[a] Alq3 experimental data from ref 16. [b] Gaq3 experimental data from ref 17. [c] B3LYP/6-31G*. [d] HF/6-31G*//B3LYP-6-31G* dipole moment.

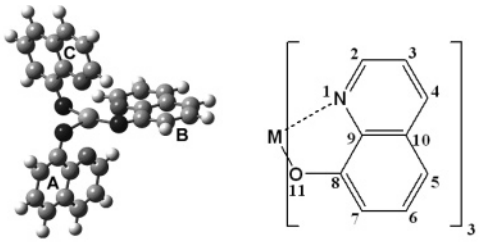

n	The different ligand	Corresponding complex
1	Quinolin-8-ol	Mq3
2	Cinnolin-8-ol	MC3
3	Quinazolin-8-ol	MZ3
4	Quinoxalin-5-ol	MX3
5	1,5-naphthyridin-4-ol	M-5N3
6	1,6-naphthyridin-8-ol	M-6N3
7	1,7-naphthyridin-8-ol	M-7N3

M = Al, Ga; n = 1: pristine complex; n = 2, 3,…,7: substituted "CH" position as labeled in the figure.

Figure 1. Model structures used (a) for the pristine molecule in which A, B, and C design the three ligands and (b) for the ligand labeling for both the substituted and pristine complexes considered in this work.

ing identical molecular shape with both Al−N and Al−O bond lengths equal to 2.04 (± 0.02 Å) and 1.84 ± (0.02 Å) respectively[2]. A detailed analysis of the M−N bond length evolution will be provided in section 3.3.

3.1.2. Electronic Structure. For Alq3, the energies of the highest occupied molecular orbital (HOMO) triplet for *mer*-Alq3 computed at the HF/6-31G*//B3LYP/6-31G* level of theory are −7.03 eV (−0.2583 au), −7.27 eV (−0.2672 au), and −7.42 eV (−0.2726 au) for HOMO, HOMO-1, and HOMO-2, respectively. These values agree well with the energy splitting predicted by the DFT-B3LYP results, with the highest level split ca. 0.24 eV (0.0088 au) from the next occupied level which is only split by about half this amount ca. 0.15 eV (∼0.0054 au)

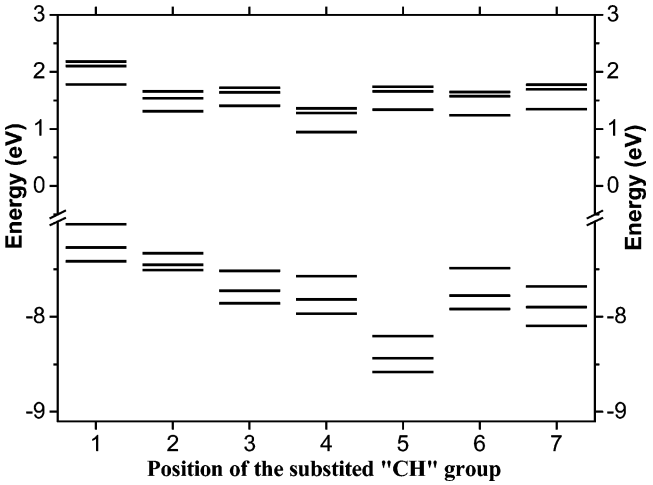

Figure 2. Evolution of the HF/6-31G* computed energies for the three highest occupied and the three lowest unoccupied molecular orbitals in the aluminum complexes.

from the last level in the triplet. The numerical value for the HOMO energy computed at the HF/6-31G* level of theory is in good agreement (by ∼0.2 eV) with recently reported experimental gas-phase ionization energy determination of 7.25 eV,[19] and this may justify the choice of the method and basis set used to predict the frontier molecular orbital (FMO) energies for the set of OLED chelates we are studying in this work. In Table 2, we list the calculated energies for HOMO and the lowest occupied orbital (LUMO) eigenvalues for the investigated ML3 complexes relative to their pristine ones (Mq3) as obtained from B3LYP/6-31G* on one hand and from HF/6-31G* single point calculations performed on the optimized structures on the other hand. For a better understanding of the influence of the substitution on the electronic structure, Figure 2 shows the evolution of the HF/6-31G* computed energies for the three highest occupied and the three LUMOs in the aluminum complexes, a similar trend being also observed for the gallium complexes.

TABLE 2: The HOMO, LUMO, and Gap Energies (E_g) Computed at HF/6-31G* and B3LYP/6-31G* for the Two Series of Complexes[a]

	HF_{EG} (au)			DFT-$B3LYP_{EG}$ (au)		
cplx	HOMO	LUMO	E_g	HOMO	LUMO	E_g
			M = Al			
Mq3	−0.2583	0.0654	0.3237 (8.808 eV)	−0.1840	−0.0637	0.1203 (3.274 eV)
MC3	−0.2695	0.0481	0.3176 (8.642 eV)	−0.2044	−0.0904	0.1140 (3.102 eV)
MZ3	−0.2763	0.0515	0.3278 (8.920 eV)	−0.2019	−0.0805	0.1214 (3.303 eV)
MX3	−0.2765	0.0327	0.3092 (8.413 eV)	−0.2020	−0.0930	0.1090 (2.966 eV)
M-5N3	−0.3001	0.0479	0.3480 (9.469 eV)	−0.2174	−0.0797	0.1377 (3.747 eV)
M-6N3	−0.2734	0.0438	0.3172 (8.631 eV)	−0.2014	−0.0849	0.1165 (3.170 eV)
M-7N3	−0.2808	0.0641	0.3449 (9.385 eV)	−0.2160	−0.0922	0.1238 (3.368 eV)
			M = Ga			
Mq3	−0.2567	0.0639	0.3206 (8.724 eV)	−0.1835	−0.0643	0.1192 (3.244 eV)
MC3	−0.2685	0.0483	0.3168 (8.621 eV)	−0.1944	−0.0788	0.1156 (3.146 eV)
MZ3	−0.2747	0.0498	0.3245 (8.830 eV)	−0.2013	−0.0812	0.1201 (3.268 eV)
MX3	−0.2765	0.0327	0.3092 (8.413 eV)	−0.2014	−0.0936	0.1078 (2.933 eV)
M-5N3	−0.3003	0.0479	0.3482 (9.475 eV)	−0.2169	−0.0802	0.1367 (3.720 eV)
M-6N3	−0.2742	0.0466	0.3208 (8.729 eV)	−0.2008	−0.0857	0.1151 (3.132 eV)
M-7N3	−0.2816	0.0481	0.3297 (8.972 eV)	−0.2053	−0.0804	0.1249 (3.399 eV)

[a] HF_{EG} = HF computed eigenvalues; DFT-$B3LYP_{EG}$ = DFT-B3LYP eigenvalues; cplx = complexes; au = atomic unit.

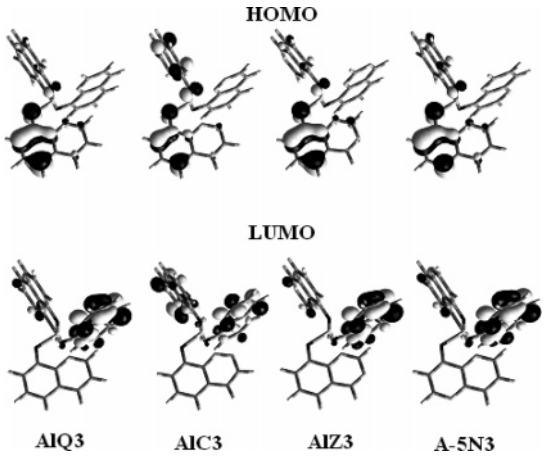

Figure 3. Molecular orbital surfaces (0.05 e au^{-3}) of the HOMO (upper panel) and LUMO (lower panel) for the *mer*-Alq3 and three of its "CH"/N substituted derivatives.

From the results presented in Table 2, it can be seen that the magnitudes of the eigenvalues and their relative differences are different for these two approaches, the main feature being not their absolute eigenvalues but the relative trend of the values. One general trend that is observed from these is that the "CH"/N substitution in the quinolinate ligand decreases (and stabilizes) HOMO and LUMO eigenvalues at the same time, owing to the presence of one more nitrogen atom (compared to Alq3) and very dependently on the position of the substituted "CH" group in the ligand.

In these two series of complexes, the HOMO shows almost the same bonding−antibonding pattern; it is localized on the residual phenoxide side (mainly on O_{11}, C_9, C_8, C_7, and C_5 atoms) of the ligand-A with a relatively significant contribution from the nitrogen atom wherever present, especially for M-5N3 (Figure 3) and M-7N3.

A relatively significant difference is however observed for AlC3 whose HOMO is found to be localized on both ligands A and B instead of ligand A (observed for the other derivatives, recalling the HOMO characters in the pristine Alq3). As a consequence of this redistribution in electron density, compared to the Alq3, electron density decreases on O_{11}, C_9, C_8, C_7, and C_5 atoms of ligand A while increasing very remarkably in ligand B. Due to the inductive effect of the nitrogen, the energy of the HOMO gets stabilized from Alq3 to Al-5N3. It is then progressively destabilized in the sequence Al-5N3 < Al-7N3 < Al-6N3 as a consequence of increased π-delocalization. Compared to that of Al-7N3, the HOMO level of Al-6N3 is stabilized.

The LUMO also shows common characteristics in the whole series: it is localized on the residual pyridyl side of ligand B with a larger contribution from the nitrogens for MC3, MZ3 (Figure 3), and MX3. For AlC3 however, the LUMO is almost uniformly localized on ligands C and B instead of ligand B as observed for the other derivatives which seem to retain the LUMO characters in the pristine Alq3. Similarly to the HOMO, the LUMO is stabilized, on going from Alq3 to AlX3, in the progressive sequence of Alq3 < AlC3 < AlX3 < AlZ3 owing to the inductive effect of the nitrogen atoms. It is then progressively destabilized in the sequence AlX3 < Al-6N3 < Al-5N3 < Al-7N3.

The greatest increase on HOMO eigenvalue (∼0.04 au with HF and ∼0.03 au with B3LYP) was obtained for M-5N3, while the smallest (∼0.011 au with HF and ∼0.02 au with B3LYP) correspond to MC3. Within the LUMO eigenvalues, the greatest decrease was observed for MX3 (∼0.03 au with both HF and B3LYP), the smallest being found for the M-7N3 compound. The net effect was found to be that, in comparison to the unsubstituted Mq3, the HOMO−LUMO energy gap decreases for MC3, MX3, and M-6N3 while increasing in the other cases.

Note that a simple NBO charge analysis of the ground-state wave function gives the metal ion charge as ca. +2.085 (±0.002) for Al (in all the Al complexes) and ca. +2.170 (±0.003) for Ga (in all the Ga complexes), well below their formal value of +3 in a simple ionic view. This feature indicates significant covalency in the metal−ligand interactions which may not be profoundly affected by the "CH"/H substitution.

3.1.3. Dipole Moment. The ground-state dipole moment (μ) values for all the compounds considered in this work, computed at both B3LYP/6-31G* and HF/6-31G* levels of theory, are given in Table 1, the general trend being plotted in Figure 4 as function of the position of the substituted "CH" group in the 8-hydroxyquinoline ligand for a clear interpretation.

From these results, it can be found that the "CH"/N substitution (in ML3 complexes) may profoundly affect μ dependently on the substituted group. In general, within the two levels of theory, μ is predicted to decrease from Alq3 to MZ3. It then progressively increases from MZ3 to M-7N3 in the sequence AlZ3 < AlX3 < Al-5N3 < Al-6N3 < Al-7N3. In

TABLE 3: B3LYP/3-21G* and CIS/3-21G* Computed Optical Properties for Al and Ga Complexes[a]

	S_0		S_1			
cplx	$\lambda^{TD-B3LYP}_{abs}$	f	λ^{CIS}_{em}	f	$\lambda^{TD-B3LYP}_{em}$	f
			M = Al			
Mq3	423 (2.93)	0.0662	331 (3.75)	0.1852	524 (2.37)	0.0453
MC3	466 (2.66)	0.0510	376 (3.30)	0.1771	596 (2.08)	0.0439
MZ3	429 (2.89)	0.0713	341 (3.63)	0.1849	549 (2.26)	0.0439
MX3	472 (2.63)	0.0536	371 (3.34)	0.1240	638 (1.94)	0.0279
M-5N3	366 (3.39)	0.0740	283 (4.38)	0.2498	424 (2.92)	0.0402
M-6N3	432 (2.87)	0.0761	335 (3.70)	0.2059	532 (2.56)	0.0445
M-7N3	397 (3.12)	0.0698	317 (3.92)	0.2178	485 (2.56)	0.0506
			M = Ga			
Mq3	426 (2.91)	0.0540	335 (3.70)	0.1856	529 (2.34)	0.0468
MC3	467 (2.65)	0.0503	382 (3.24)	0.1755	606 (2.05)	0.0435
MZ3	433 (2.87)	0.0355	346 (3.59)	0.1851	556 (2.23)	0.0440
MX3	477 (2.60)	0.0401	376 (3.30)	0.1246	645 (1.92)	0.0281
M-5N3	367 (3.38)	0.0759	286 (4.34)	0.2510	426 (2.91)	0.0665
M-6N3	435 (2.85)	0.0677	339 (3.66)	0.2062	536 (2.31)	0.0517
M-7N3	399 (3.11)	0.0740	320 (3.87)	0.2184	488 (2.54)	0.0578

[a] cplx = complexes; f = oscillator strength; λ_{abs} = maximum absorption wavelength; λ_{em} = maximum emission wavelength; the values in parentheses are the corresponding absorption/emission energies in eV.

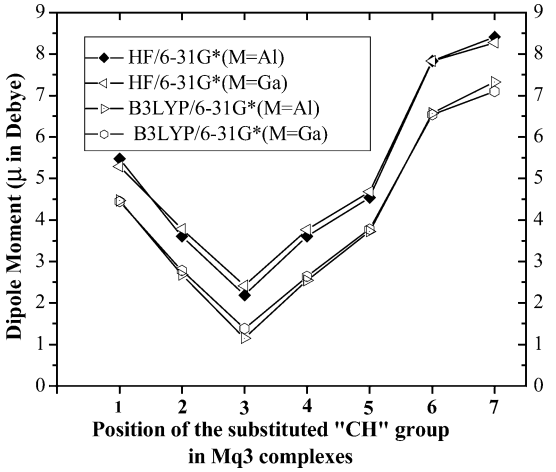

Figure 4. The effect of the "CH"/N substitution on the dipole moment (μ) in the ML3 chelates (M = Al, Ga) computed at both HF/6-31G* and B3LYP/6-31G* levels.

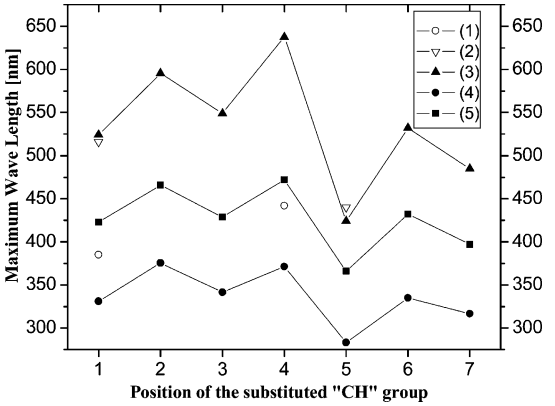

Figure 5. TDB3LYP/3-21G* calculated max absorption (5) and emission wavelengths (3), CIS/3-21G* calculated emission wavelength (4) for Alq3 and its derivatives (corresponding to $n = 1-7$ as defined in Figure 1). Experimental data for Alq3 and M-5N3 are plotted by (2) for λ_{em} and (1) for λ_{ab}.

comparison to Alq3, μ was predicted to increase (by 2−3 D) when the substitution occurs on positions 6 and 7 and to decrease in the other cases, the greatest (>3 D) and smallest (<1 D) decreases being observed for the MZ3 and M-5N3 complexes, respectively.

3.2. The First Excited State and Photophysical Properties. In Table 3, we summarize the calculation results for the first singlets excitation energies with the corresponding oscillator strengths based on TD-B3LYP and CIS calculations using 3-21G* basis set (Table S1 for 6-31G results, Supporting Information). It is shown that the tuning of emitting color can be reached by changing the position of N in the 8-hydroxyquinoline ligand. For a better interpretation, the trends of the results discussed in this paragraph are plotted in Figure 5 for Al complexes (similar trends being found also for Ga complexes) showing an important red shift of the absorption spectra of ca. 40 and 50 nm, for MC3 and MX3, respectively, their emission spectra being red shifted by ca. 74 and 111 nm, respectively. On the other side, a remarkable blue shift of ca. 60 and 28 nm was predicted, for M-5N3 and M-7N3 λ_{abs}, respectively, while for the same chelates, an important blue shift of ca. 106 and 43 nm was predicted for their λ_{em} (See also Figure S2). In general all these results reflect the trends of the eigenvalue differences discussed in the previous section.

Over the series, the first optical transition corresponds mainly to a HOMO → LUMO excitation (See Table S2). It evolves as the HOMO−LUMO gap and therefore reflects the changes in electronic structure described above (Figure 3). Although TD-B3LYP/3-21G* chemical model tends to underestimate this property for Alq3, Gaq3, AlX3 whose predicted values are 2.93 eV (422.99 nm), 2.91 eV (426.34 nm), and 2.63 eV (472.19 nm), it is interesting to note its good ability to predict the observed absorption red shifts. Indeed, the experimental red shift of ∼4−5 nm, i.e., respectively 385 nm [4] (in chloroform)/386 nm [20] (in DMSO) and 390 nm [20] (in DMSO), is predicted to be ∼4 nm with both TD-B3LYP/3-21G* and TD-B3LYP/6-31G. On going from Alq3 to AlX3 whose maximum absorption wavelength (λ_{ab}) in chloroform is reported to be 442 nm,[4] the experimental red shift of 57 nm is also predicted within ∼7 nm (i.e., ca. 50 nm) of agreement.

Wherever available, the computed emission wavelengths (λ_{em}) agree well with experimental data, particularly with the experimental values of 510−516 nm[21,22] and 525−529 nm[21−23] for Alq3 and Gaq3, respectively, where excellent agreement was obtained not only for the λ_{em} numerical values but also for the shape of the experimental emission spectra[22] (Figure S1). For most of the derivatives of interest in this study, a few experimental data can be found in the literature except for M-5N3 whose PL is reported at 440 nm[2] (i.e., blue-shifted by

ca. 90 from that of Alq3). Interestingly, a sufficiently good agreement can be observed between our computational result (~424 nm) and the experimental M-5N3 PL value and this, combined to the excellent agreement between the TD-B3LYP/3-21G* and experimental values already obtained for Gaq3 and Alq3, gives credit to the computational approach. For AlX3 however, both the TD-B3LYP/3-21G* and TD-B3LYP/6-31G predicted values are found to overestimate the reported PL red shift of ~60 nm relative to Alq3 (i.e., ~580 and 520 nm, respectively).[4] Under the hypothesis that this may have been caused by an inability of the basis set used to optimize the S1 structure, the 3-21+G** successfully used by Halls and Schlegel[24] in the study of the first excited state for Alq3 was used within TD-B3LYP/3-21+G**//CIS/3-21+G** to recalculate λ_{em} for AlX3; no improvement was however provided toward the reported value. Therefore, we thought that the source of the disagreement between the reported value and the one provided by our calculations may not be ascribed to the computational approach adopted in this study. In all cases, a qualitative agreement can be found between the predicted optical properties and available experimental as well as theoretical data where available. Moreover, even on the quantitative point of view, most of the results agree well with available experimental data except for M-5N3 λ_{em}.

Experimentally, it has been proven that Gaq3 based OLED has not only greater luminescent brightness but also higher quantum efficiency than the Alq3 based one.[25] Neither the CIS nor TD-B3LYP calculated *f* values associated to the simulated λ_{em} values listed in Table 3 do sufficiently favor the former property, with a very little difference being observed between the Gaq3 and Alq3 *f* values, the greatest being however observed for the former. In most of the ML3 derivatives (where M = Al, Ga, and L is one of the seven ligands), except for AlC3 whose *f* value associated to the predicted λ_{em} are greater for GaC3 than for its analogue AlC3, our computational results are consistent with a greater *f* for GaL3 than their homologue AlL3, the greatest differences (Δf = ~0.04 and ~0.02 respectively for CIS and TDB3LYP) being observed between the 5-substituted 8-hydroxyquinoline Ga and Al derivatives. Hence it would appear that with the same ligand, GaL3 complexes would photoluminese with the greatest intensity compared to the AlL3 ones. The results strongly suggest that the "CH"/N substitution should have a certain effect on Δf between GaL3 and AlL3 chelates depending on the position of the substituted group, the most important difference being found when the substitution concerns the phenoxyl side of the 8-hydroxyquinoline.

3.3. The Metal−Ligand Bonding Nature and Optical Spectra Shifts in the "CH"/N Substituted Gaq3 and Alq3 Derivatives: Should They Be Correlated? In the "CH"/N substituted derivatives of interest in this contribution, we have been interested in the new look of the covalent nature of the metal−ligand and the correlation that could exist between the spectral shifts we discussed above and the induced structural shift. In Figure 6, we plotted for a clear interpretation, the calculated changes in M−N bond lengths relative to the pristine Mq3 in case of Al−N bond length (for Al complexes).

In Figure 6, the negative and positive values correspond to the shortening and lengthening of the M−N bond, respectively, from which one may deduce the effect of the "CH"/N substitution on the bond strength. In general, relative to Mq3, the M−N bond length is found to be perturbed as follows: M−N_A bond is lengthened in MZ3, MX3, and M-6N3 and shortened in the three other cases; M−N_B lengthening is observed in MZ3, MX3, M-6N3, and M-7N3 and its shortening is observed in the other two cases while M−N_C bond is found to be lengthened in all the cases except for M-5N3 and M-7N3. Even if no general rule can derive from these results, an interesting feature that was observed is that the main important red and blue shifts predicted correspond to the cases where the three M−N bonds are affected in the same direction, i.e., lengthened or shortened at the same time (see AlZ3 and AlX3 for red shift and Al-5N3 for blue shift). For the other three derivatives, one M−N bond is lengthened while the two others are shortened (MC3 and M-7N3) or vice versa (M-6N3). On the basis of these results, the difference in red shift observed for AlZ3 and AlX3 compared to Alq3 fluorescence spectrum can also be well explained by the net difference observed in the magnitude of their M−N bond lengthening.

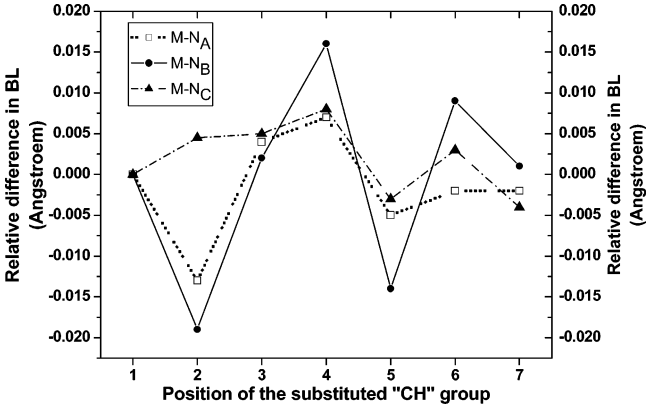

Figure 6. The effect of the "CH"/N substitution on the Al−N bond length (BL) compared to Alq3.

TABLE 4: NBO Charges on N and M Atoms in the Two Series on Complexes Calculated at HF/6-31G Level Starting from the B3LYP/6-31G* Ground (S_0) State Optimized Geometries

selected atom	Mq3	MC3	MZ3	MX3	M-5N3	M-6N3	M-7N3
			M = Al				
N_A	−0.615	−0.354	−0.650	−0.567	−0.623	−0.624	−0.604
N_B	−0.627	−0.371	−0.664	−0.578	−0.635	−0.636	−0.616
N_C	−0.627	−0.374	−0.662	−0.581	−0.633	−0.638	−0.618
Al	2.172	2.168	2.170	2.169	2.169	2.170	2.167
			M = Ga				
N_A	−0.618	−0.361	−0.654	−0.566	−0.623	−0.622	−0.608
N_B	−0.637	−0.374	−0.674	−0.583	−0.641	−0.641	−0.626
N_C	−0.627	−0.370	−0.662	−0.576	−0.631	−0.638	−0.619
Ga	2.086	2.087	2.085	2.083	2.085	2.085	2.084

Table 4 shows electron population changes on the atoms involved in the M−N bond (N, Al, and Ga), where the NBO method[25] was applied to the HF/6-31G//B3LYP/6-31G* ground state. Negligibly small changes in electron population are observed for both Al and Ga in the two series of complexes relative to the pristine ones, while some remarkable changes are predicted for the N atom. This clearly indicates that the M−N length shift may be due to the electron population repartitioning occurring over the ligand remaining the metal atom almost unaffected. Compared to other complexes, an analyses of both NBO and Mulliken populations are consistent with a dramatically reduced N population (both the substituting and the metal linked nitrogen) of MC3 (see Figure S4). Recalling the uncommon electronic structure revealed by this study for MC3, whose HOMO and LUMO were equally localized on two of the three ligands, such uncommon behaviors only observed for MC3 may be ascribed to the −N═N− bond which is absent in the other cases.

From a careful analysis of both calculated and available experimental M−N bond length in different Mq3-like (M = Al, Ga, In) chelates,[17,18,26] the general tendency is that with reference to the parent 8-hydroxyquinolinate Al, the three M−N bonds are consecutively lengthened or shortened depending on the cases. Hence, it should be reasonable to expect a $M-N_C$ shortening for MC3, $M-N_A$ lengthening for M-6N3, and $M-N_C$ shortening for M-7N3 which are predicted out of the general trend (see Figure 6) using B3LYP/6-31G*. We believe, based on the findings resulting from our previous investigation of the basis set effect on a set of Gaq3 properties,[27] that better accuracy may be attainable using the same functional by additional augmentation with diffuse functions to the 6-31G* basis we used in structural optimizations. It is clear however from our calculation results, particularly for MZ3, MX3, and M-5N3, that fluorescence spectral shifts can be correlated to the M−N BL shift compared to the ML3 compound parents, a fact that was also reported for similar aluminum complexes.[28]

4. Summary and Conclusions

From this theoretical study, some light was shed on the "CH"/N substitution effect on the fluorescent Alq3 and Gaq3 structures and properties: (i) B3LYP/6-31G* calculations indicated some small structural changes in the parameters involving the metal atom namely the M−N bond lengths which were correlated to the experimental and theoretical spectral shifts. (ii) Both HF/6-31G* and B3LYP//6-31G* predictions are consistent with the HOMO and LUMO stabilization whose net impact can be either an increasing or decreasing of the E_g depending on the position of the substituted "CH" in the ligand. (iii) On the basis of TD-B3LYP/3-21G*(6/31G)//CIS/3-21G*-(6-31G) calculated emission energies which match closely the trend of the eigenvalue differences, a relatively significant blue (red) shift owing to the "CH"/N substitution in positions 2 and 4 (5 and 7) in the quinolinate ligand was predicted for AlL3 and GaL3, the greatest corresponding to 4- and 5-substituted 8-hydroxyquinoline derivatives, respectively. Therefore, the tuning of different emitting color for ML3 complexes can be reached by the different position "CH"/N substitution on ligands. (iv) With reference to the parent compounds, the dipole moment was predicted to be profoundly affected the most important change being found when the CH"/N substitution occurs on the phenoxyl side of the ligand.

Acknowledgment. Financial support from the NNSFC (No. 50473032), SRF for ROCS, SEM, and Outstanding Youth Project of Jilin Province are gratefully acknowledged.

Supporting Information Available: Simulated fluorescence spectra for Alq3 together with its Al/Ga and "CH"/N substituted derivatives; detailed data providing all the TDB3LYP/3-21G*, CIS/3-21G*, B3LYP/6-31G, and CIS/6-31G results not given in the text; HF/6-31G calculated Mulliken and NBO charges. This material is available free of charge via the Internet at http://pubs.acs.org.

References and Notes

(1) Chen, C. H.; Shi, J. M. *Coord. Chem. Rev.* **1998**, *171*, 161.
(2) Van Slyke, S. A.; Bryan, S. P.; Lovencchio, F. V. US Patent 5, 150, 1990.
(3) Burrows, P. E.; Shen, Z.; Bulovic, V.; McCarty, D. M.; Forrest, S. R.; Crinin, J. A.; Thompson, M. E. *J. Appl. Phys.* **1996**, *79*, 7991−8005.
(4) Becke, A. D. *J. Chem. Phys.* **1993**, *98*, 5648−5652.
(5) Lee, C.; Yang, W.; Parr, R. G. *Phys. Rev.* **1988**, *B41*, 785−789.
(6) Stephens, P. J.; Devlin, F. J.; Chabalowski, C. F.; Frisch, M. J. *J. Phys. Chem.* **1994**, *98*, 11623−11627.
(7) Hariharan P. C.; Pople, J. A. *Mol. Phys*. **1974**, *27*, 209.
(8) Gordon, M. S. *Chem. Phys. Lett*. **1980**, *76*, 163.
(9) Frisch, M. J.; Pople J. A.; Binkley, J. S. *J. Chem. Phys*. **1984**, *80*, 3265.
(10) Foresman, J. B.; Head-Gordon, M.; Pople J. A.; Frisch, M. J. *J. Phys. Chem.* **1992**, *96*, 135−149.
(11) Binkley J. S.; Pople J. A.; Hehre W. J. *J. Am. Chem. Soc.* **1980**, *102*, 939.
(12) Gordon M. S.; Binkley J. S.; Pople J. A.; Pietro W. J.; Hehre W. J. *J. Am. Chem. Soc*. **1982**, *104*, 2797.
(13) Frisch M. J.; Pople J. A.; Binkley J. S. *J. Chem. Phys*. **1984**, *80*, 3265.
(14) Frisch, M. J.; Trucks, G. W.; Schlegel, H. B.; Scuseria, G. E.; Robb, M. A.; Cheeseman, J. R.; Zakrzewski, V. G.; Montgomery, J. A.; Stratmann, R. E.; Burant, J. C.; Dapprich, S.; Millan, J. M.; Daniels, A. D.; Kudin, N.; Strain, M. C.; Farkas, O.; Tomasi, J.; Barone, V.; Cossi, M.; Cammi, R.; Mennucci, B.; Pomelli, C.; Adamo, C.; Clifford, S.; Ochterski, Petersson, G. A.; Ayala, P. Y.; Cui, Q.; Morokuma, K.; Malich, D. Rabuck, A. D.; Raghavachari, K.; Foresman, J. B.; Cioslowski, J.; Ortiz, V.; Baboul, A. G.; Stefanov, B. B.; Liu, G.; Liashenko, A.; Piskorz, Komaromi, I.; Gomperts, R.; Martin, R. L.; Fox, D. J.; Keith, T.; Al-Laham, M. A.; Peng, C. Y.; Nanayakkara, A.; Gonzales, C.; Challacombe, M.; Gill, P. M. W.; Johnson, B.; Chen, W.; Wong, M. W.; Andreas, J. L.; Head-Gordon, M.; Reploge, E. S.; Pople, J. A. *Gaussian 98*; Gaussian Inc.: Pittsburgh, PA, 1998.
(15) Brinkmann, M.; Gadret, G.; Muccini, M.; Taliani, C.; Masciocchi, N.; Sironi, A. *J. Am. Chem. Soc.* **2000**, *122*, 5147.
(16) N. M. O'Boyle and J. G. Vos, Gauss Sum 0.8, Dublin City University, **2004**.
(17) Wang, Y. W.; Li, Y.; et al. *Chem. Mater.* **1999**, *11*, 530−532.
(18) Slattery, D. K.; Linkous, C. A.; Gruhn, N. *Polym. Prepr.* **2000**, *41*, 866.
(19) Ghedini, M.; Deda M. L.; Aiello, I.; Grisolia, A. *Synth. Met.* **2003**, *138*, 189−192.
(20) Yasuharu, N.; Keizo, H.; Kiyotoshi, M.; Koichi, T.; Tsunenobu, S.; Taro, N. *Inorg. Anal. Chem.* **1976**, *25*, 459−63.
(21) Li, H. R.; Zhang, F. J.; Wang, Y.Y.; Zheng, D. S. *Mater. Sci. Eng., B* **2003**, *100*, 40−46.
(22) http://www.adsdyes.com.
(23) Wang, L. J.; Jiang, X. Y.; Zhang, Z. L.; Xu, S. H. *Displays* **2000**, *21*, 47.
(24) Halls, M. D.; Schlegel, H. B. *Chem. Mater*. **2001**, *13*, 2632.
(25) Reed, A. E.; Curtiss, L. A.; Weinhold, F. *Chem. Rev*. **1988**, *88*, 899.
(26) Sapochat, L. S.; Ranasinghe, A.; Kohlmann, H.; Ferris, K. F.; Burrows, P. E. *Chem. Mater*. **2004**, *16*, 401.
(27) Gahungu, G.; Zhang, J. P. Molecular geometry, electronic structure and optical properties. study of meridianal tris(8-hydroxyquinolinato)-gallium(III) with ab initio and DFT methods. *J. Mol. Struct.: Theochem*, in press.
(28) Hong-Ze, G.; Zhong-Min, S.; Chun-Sheng, Q.; Ri-Gen, M.; Yu-He K. *Int. J. Quantum Chem.* **2001**, *97*, 992−1001.